Measurement 175 (2021) 109099

Contents lists available at ScienceDirect

Measurement

journal homepage: www.elsevier.com/locate/measurement

Strain and displacement measurement based on distributed fibre optic sensing (DFOS) system integrated with FRP composite sandwich panel

Maciej Kulpa [a], Tomasz Howiacki [b,c,*], Agnieszka Wiater [a], Tomasz Siwowski [a], Rafał Sieńko [b]

[a] Faculty of Civil and Environmental Engineering and Architecture, Rzeszow University of Technology, al. Powstancow Warszawy 12, 35-959 Rzeszow, Poland
[b] Faculty of Civil Engineering, Cracow University of Technology, ul. Warszawska 24, 31-155 Krakow, Poland
[c] SHM System Company, Jana Pawla II 82A Libertów, 30-444 Krakow, Poland

ARTICLE INFO

Keywords:
Distributed fibre optic sensors
Rayleigh scattering
Strain and displacement measurements
FRP bridge deck panel
Testing validation
Smart structures

ABSTRACT

An increase in application of advanced materials and high-tech monitoring systems is being observed in bridge engineering in recent years. The main goal is aimed at optimizing maintenance costs spent during entire lifecycle of a bridge. The paper describes the concept of the smart fibre reinforced polymer (FRP) sandwich deck panel, dedicated for newly-designed and renovated bridges. This panel is equipped with the distributed fibre optic sensing (DFOS) system, integrated with composite laminates. The DFOS system is provided to control strain and displacement measurement, further used in the structural health monitoring of a bridge. The DFOS system is characterized by the following features: accurate, reliable and distributed strain measurements, possibility of assessing shape and displacements, detection of local damages, reliable protection of the sensors, no need for surface installations, high durability, measurements from the real zero state of the structural element. Exemplary results of distributed fibre optic strain and displacement measurements performed under laboratory conditions on laminate specimens as well as the beam cut from the prototype panels are presented and compared to conventional measurements and FEM predictions.

1. Introduction

In the last 40 years since the early 1980s, fibre reinforced polymer (FRP) composites have been used in many bridge applications due to their excellent strength, weight and durability characteristics [1,2,3,4]. There are many benefits of FRPs, which encourage bridge designers to use this material in many structural forms. The benefits could be summarized as: weight saving (high strength to weight ratio, light-weight), low maintenance requirement, resistance to the environment effects (corrosion-free), ability to be formed into a complex shape and easy to install offsite engineered and fabricated elements. Thanks to their properties they could be tailored to the requirements of applications with complex shape [5,6,7,8].

All FRP composite bridges have been in service as complete load bearing superstructures on public roads worldwide for over 20 years [5]. The vast majority of these all-composite bridges is performing well, although there have been a few instances where they have created problems for the bridge owner and were taken out of the service. FRP structures and components are highly susceptible to damage due to delamination, matrix cracking, inter-laminar fracture and debonding, all of which have potential to cause catastrophic structural failure. Therefore, as with any structural elements used for bridge structures, it is necessary to be able to inspect FRP structural elements. FRP materials, because of their microstructure, tend to deteriorate in ways that are not easily detected by visual examination. Therefore, in some instances the visual inspection is supplemented by various nondestructive evaluation (NDE) methods [9,10,11]. Moreover, many of existing FRP composite bridges are still being monitored to evaluate service performance of this emerging technology [12,13,14,15]. Ongoing works should be verified in situ, but also under laboratory conditions using other innovative measurement techniques, such as machine vision or image processing [16,17,18].

Nowadays, there are many efficient measurement solutions which could be successfully applied for strain and displacement measurements of bridge structures or their structural components. For long-term structural health monitoring (SHM) systems, vibrating wire technology has found a wide application due to its proven long-term stability [19], resistance to harsh environmental conditions, laboratory resolution and accuracy, as well as its versatility in measuring different physical quantities.

* Corresponding author.
E-mail address: howiacki.tomasz@gmail.com (T. Howiacki).

https://doi.org/10.1016/j.measurement.2021.109099
Received 15 June 2020; Received in revised form 4 December 2020; Accepted 23 January 2021
Available online 5 February 2021

There are also new techniques worth mentioning, which are nowadays constantly developed and improved. The important group are both microelectromechanical (MEMS) [20] and nanoelectromechanical systems (NEMS) [21], which could be successfully apply as strain, displacement, pressure, temperature, flow, acceleration, acoustic or gas sensors [22]. Also, capacitive sensors should be examined as a tool for structural monitoring. Such sensors use micro/nanobeams [23], plates or membranes to detect extremely small changes in measured physical quantity.

However, all the above-mentioned technologies have some limitations in the context of long-term structural health monitoring of bridge components. First of all, they measure physical quantities only in one single point of the structure so they are not able to direct damage detection. Secondly, they cannot be installed inside the composite laminates due to the relatively large dimensions of the final measurement set. What is more, they require the signal cables to be lead from any single sensor what would be very problematic in practical applications for large elements, like bridge slabs with an area usually over 200 m^2.

One of the main demands for the structural monitoring systems is the ability to detect damages or local abnormalities in structural behaviour [24]. However, using conventional spot sensors this task is impossible to be directly realized, even using advanced mathematical algorithms or finite element models. Usually detailed analysis is being performed to provide the optimal arrangements of the limited number of sensors within the structure. However, there is still no possibility to directly indicate the place and the reason of damage occurrence, but only general information about the changes in structural behaviour. Analysing the strain (or stress) level in particular measuring points, special care must be taken as the accuracy of the sensor position is of the great importance for the data interpretation.

Therefore, new measurement techniques and solutions are being constantly sought and developed to provide as much comprehensive and reliable information as possible with simultaneous financial feasibility. Currently, the most promising technique meeting described requirements is the distributed fibre optic sensing (DFOS) [25,26]. This approach allows to measure different physical quantities, e.g. strains [27], displacements and shape [28,29] as well as temperature [30] along the entire length of the optical fibres or sensors [31]. Distributed sensing enables effective replacement of thousands of traditional strain gauges with a single optical fibre or sensor [32]. The comparison between conventional spot measurements and the distributed ones is presented schematically in Fig. 1. DFOS offers completely new and breakthrough possibilities in the analysis and assessment of the technical condition of civil engineering structures or structural members made of different materials, e.g. steel [33], concrete [31] or FRP composite [34,35]. Both DFOS and SHM methods were originally dedicated and implemented in the space industry. Nowadays, they are intensively developed as measurement methods for composite structural elements [36].

Considering the worldwide recognized advantages of the DFOS as measuring technique in the SHM of the FRP bridges and its unique ability to measure the strain, deflection and temperature distributions along the entire length of the bridge superstructure, it was as the basic SHM system of the first Polish FRP composite bridge [37]. The validation of the DFOS technique is critical to address the development of monitoring system with improved accuracy and spatial resolution tailored for the FRP bridge application. The effectiveness of DFOS technique was evaluated through scaled laboratory experiments on a smart composite deck panel to be implemented in the FRP bridge. This paper presents a pilot application of DFOS technique to measure strains and deflections of the FRP laminate specimens and FRP beam subjected to axial tension and three-point bending, respectively. The validation through axial and bending tests and finite element analysis was performed to ensure the accurate and reliable DFOS readings. The DFOS strain profiles were first compared with spot strain measurement results and then converted into deflection profiles and validated against spot deflection measurements performed with a common inductive LVDT transducers. The additional validation based on comparison of the strain profiles with the results of three-dimensional finite-element analysis (FEA) of the FRP beam was also performed. Factors that may affect measurement accuracy are discussed on the basis of the experimental and numerical results.

2. The idea of smart FRP composite deck panel

Based on the comprehensive literature review and authors' personal experience [38], the concept of a smart FRP composite deck panel, dedicated for newly-designed and renovated bridges, was elaborated. This FRP sandwich deck panel, manufactured in the VARTM (vacuum assisted resin transfer moulding) infusion process, consists of:

- multilayer lower and upper FRP laminates (faces),
- polyurethane foam (PUR) core placed between faces,
- optional concrete core used to enable panel's mechanical connection to bridge beams or girders,
- vertical laminated ribs in the core (distributed in the form of honeycomb), connecting the faces,
- the system of longitudinal and transverse optical fibres for distributed strain and temperature measurements, integrated with faces.

The main load-bearing component of the bent panel are external faces, which are reinforced with several alternating layers of fibers:

- unidirectional, U-E,
- bidirectional with 0/90° orientation, B-E,
- and bidirectional with ±45° orientation, X-E.

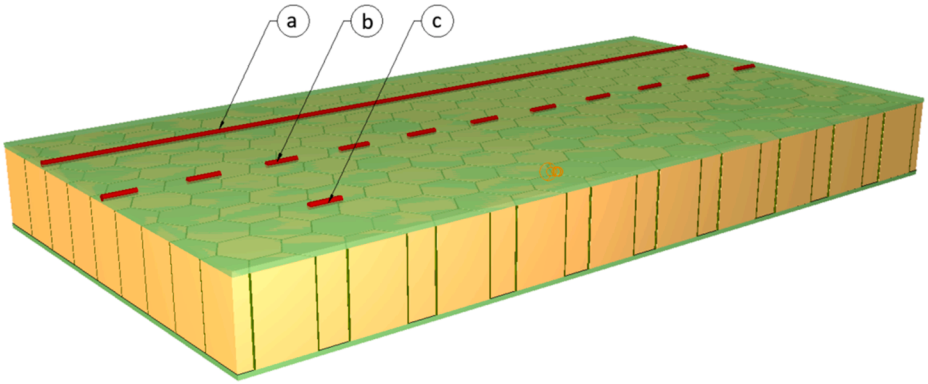

Fig. 1. The idea of measurements: a) distributed; b) quasi-distributed; c) spot.

The external laminates are connected with vertical, internal ribs, reinforced with fibres B-E and X-E. Detailed stack sequences are presented in the Fig. 2.

Fig. 3 shows the conceptual structure of the FRP panel, in which optical fibres were integrated inside the face laminates during infusion. Owing to similarity of the optic sensors and FRP composite reinforcement (glass fibres in both cases) the integration is fully possible.

Owing to integrated optic fibres smart composite panel is able to detect the bridge overloading as well as to monitor the structural health during long-term operation. Although integration of optical fibres with composite components and the creation of smart structural members were previously described in literature [39,40,41], in bridge engineering spot sensors (e.g. foil resistance or vibrating wire gauges) installed on the surface of structural elements are still commonly used. Appropriate integration of the optic fibres with the multi-layered composite laminates during their manufacturing in the infusion process provides many advantages over spot conventional measurement:

- DFOS system become an integral part of the element, so there is no need for sensor installation on the previously prepared substrate;
- strain transfer from FRP laminate to the measuring fibre is naturally provided (optic fibre is fully integrated with composite laminate during production), so obtained strain data is very accurate and reliable;
- durability of DFOS system is comparable to the designed lifetime of the monitored structure;
- composite laminate protects the optic sensors from mechanical damages or hard environmental conditions;
- initial readings can be performed during manufacturing, so that all important phenomena can be taken into account during field measurement (e.g. dead-weight or residual stress);
- appropriate arrangement of integrated fibres enables to calculate deformations (displacements) of the element;
- there is no need to select more important locations of measurement, because the entire length of the element can be monitored.

3. Distributed fibre optic sensing system

3.1. Selection and calibration of optical fibre

DFOS technique creates great opportunities, but to take its full advantage it is necessary to provide appropriate sensors or fibres as well as installation methods, which allow for accurate strain transfer from the monitored element to the measuring fibre core. The following key aspects should be taken into account:

- the best possible integration of the sensor with the element [42],
- the maximum possible reduction of slippage phenomena within the sensor itself (e.g. between particular layers or coatings) – in many cases it could be done by applying the fibres only in their primary coatings,
- the maximum strain that the fibre can withstand (particularly important when local events can occur causing extremely high value of strains),
- appropriate stiffness of the sensor [43], not to strengthen or to reinforce the element (otherwise the impact of the sensor presence should be taken into account during analysis of strain results),
- precision in arranging the optic fibre traces during installation.

Because of the necessity of integration the optical fibres inside the composite laminate, only fibres in their primary coatings could be applied thanks to their minimal dimensions (external diameter equal to 250 μm – see Fig. 4). This solution has also another advantage: the sensor will not influence the behaviour of the composite, regardless the laminate thickness.

Some mechanical parameters of the optical fibres strongly depend on the type of the primary coating, for example maximum strain range or minimum bending radius. Thus, before choosing the final solution, several different types of optical fibres and their coatings were tested during axial tensile test (Fig. 5a). Fibres were tensioned until they broke and strains were simultaneously measured by backscatter reflectometer (see also chapter 3.3) and controlled by the reference strain measurement technique. Analysing obtained data (Fig. 5b), the following rule can be observed: the stiffer the coating, the smaller the strain measuring range. Thus, the standard telecom fibre in soft acrylic coating was selected for applying in smart composite panel, which can be successfully tensioned to over 5%.

3.2. Sensors installation during manufacturing

All composite specimens described hereafter were manufactured during VARTM infusion process. Several 1.25 × 1.25 m laminates and full-scale panels were manufactured to be used for test specimens. The first step of optical fibres installation was to stabilize them along designed traces in the particular fabrics of the laminate. For this purpose, an aerosol glue was used, which allowed for spot stabilisation and slight pretension of the optical fibre. This was extremely important for ensuring straightness of measurement traces and their compliance with measurement program. Another problem was to elaborate ways to put the optical fibre outside the laminate. The use of Teflon protection tubes or embedded connectors for this purpose are known from the literature [44]. Two different approaches were elaborated in the frame of this project:

- enabling the optical splice to be done before installation and infusion process,
- high-temperature glass tubes enabling the splice to be done after installation and infusion process.

In both cases the area near the laminate edge, where the fibres went out of the specimen, has to be protected and sealed with butyl rubber tape. This enabled the infusion process to be carried out correctly and also minimised the risk of fibre mechanical damage due to sudden

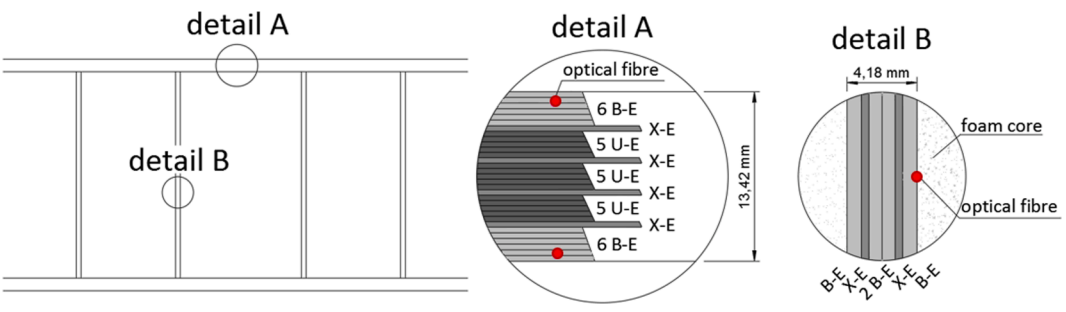

Fig. 2. Stack sequences of fibres in laminates.

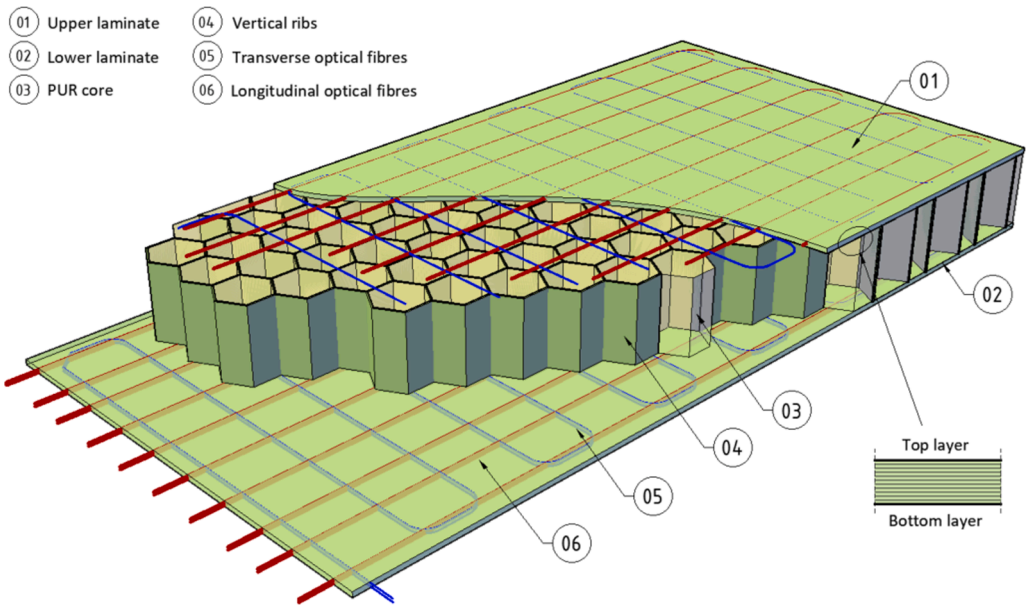

Fig. 3. The concept of smart composite panel for bridge construction, integrated with distributed fibre optic sensing system.

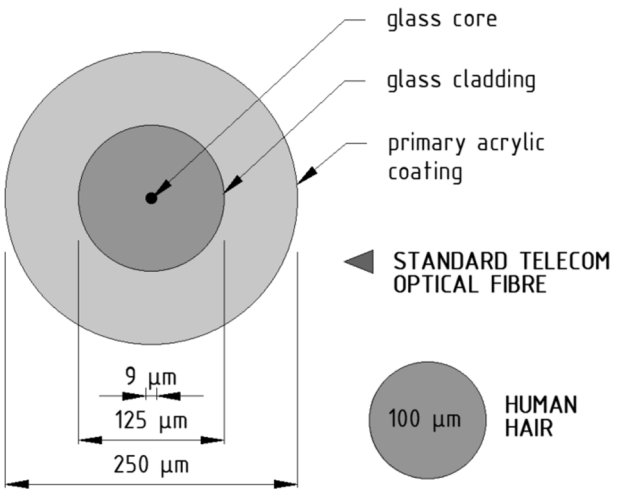

Fig. 4. Cross-section of the standard telecom optical fibre SM9/125 type in its primary coating.

stiffness change. Fig. 6a shows the arrangement of optical fibres on one of the fabrics of the multi-layered laminate. In this case high temperature glass tubes were used to protect the fibres within the laminate's edge area. In turn, Fig. 6b shows the standard telecom pigtails spliced before installation, coming out from the composite panel during its infusion.

Two methods of the fibres termination were also proposed, depending on the kind of the specimen. The first one consisted of splicing the pigtails on both sides of the fibre and shaping the fibre in the loop. This method minimizes the risk of losing information in case of the fibre breakage, as it allows the measurement to be performed from both sides of the fibre. However, more pigtails coming out from the laminate hamper the installation and infusion process and cannot be used for low-scale specimens. In such cases, the high attenuation terminations were made and successfully testes, e.g. in the form of a very small radius loop or a splice with modified attenuation parameters.

After the infusion process was completed, the ready laminates and panels were cut into the smaller specimens dedicated for different type of testing, i.e. the axial tensile tests of the laminate specimens as well as the three-point bending test on the beam specimen.

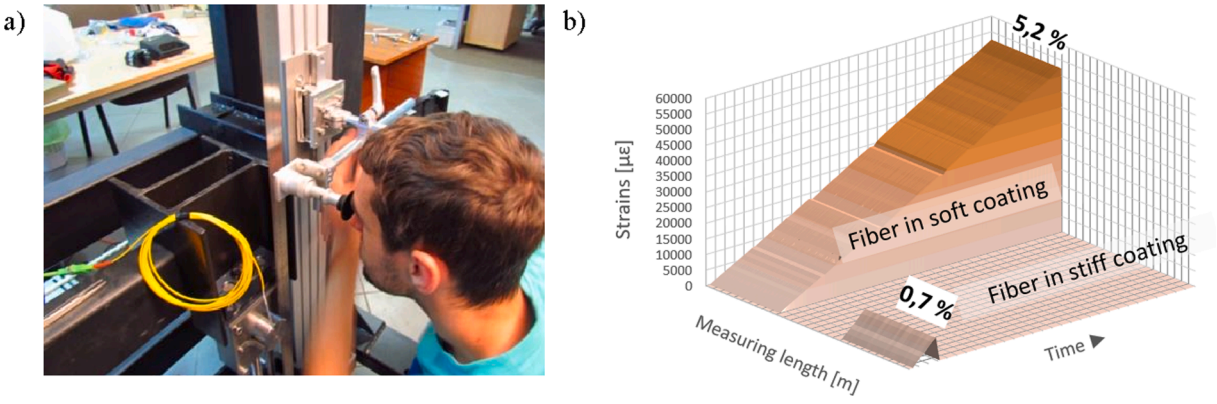

Fig. 5. Axial tensile test of optical fibres: a) the view of reference microscope technique applied; b) exemplary results showing the differences in measuring range depending on the stiffness of the primary coating of the fibre.

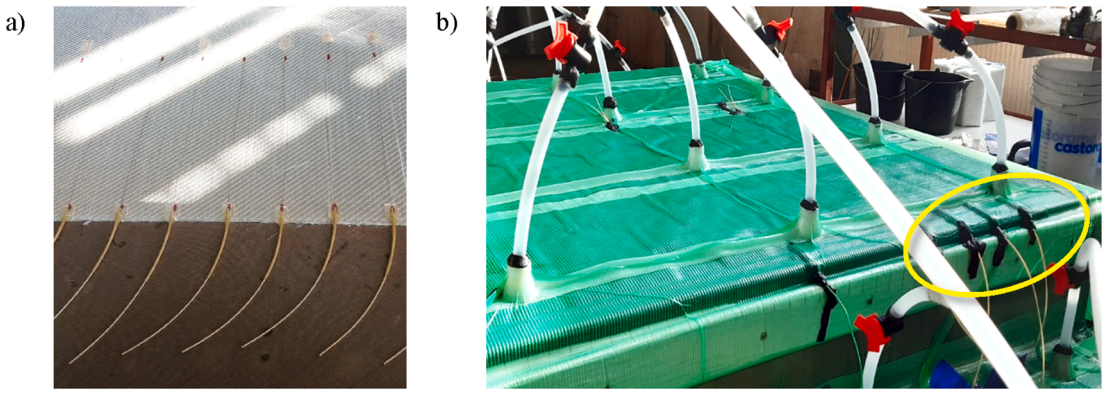

Fig. 6. Two approaches of coming the optical fibre out of laminate: a) arrangement of the optical fibres over one of the fabrics of the multi-layered laminate with high temperature glass tubes; b) standard telecom pigtails coming out the composite panel during infusion.

3.3. Rayleigh backscattering and measuring parameters

In telecommunication applications the aim is to make the glass fibres as clean and pure as possible, i.e. free of imperfections, microcracks, micro-pollution or local changes in density, which cause decreasing the signal power with the length of the fibre [45]. One of the reasons is the Rayleigh scattering phenomena [46], which occurs in each section of the fibre as a result of the partial structure of matter, causing the fluctuations in the local refractive index. This is accompanied by backscattering in the sense that the light wave reflected from the imperfections of the glass structure moves backwards in relation to the original direction of movement (Fig. 7a). The dispersion amplitude is a random but constant property for a given fibre (Fig. 7b). It could be compared to the unique fingerprint of the given optical fibre [47]. Nowadays, the analysis of this phenomena is performed using advanced optical reflectometers or interrogators.

If mechanical or thermal strains change along the length of the fibre, the distances between local imperfections will also be changed. It is visible as a frequency shifts within the Rayleigh signal between two subsequent measurements. The current scatter profile is compared with the reference profile to calculate mechanical or thermal strains with extremely high, mm-order spatial resolution. It should be noted that within a single optical fibre, using only one scattering-based device, it is not possible to separate the strains resulting from mechanical loads and temperature changes [48]:

$$\frac{-\Delta \upsilon}{\upsilon} = K_T \cdot \Delta T + K_\varepsilon \cdot \Delta \varepsilon \tag{1}$$

where

- υ – mean optical frequency (Hz),
- K_T – temperature calibration constant (°C^{-1}),
- K_ε – strain calibration constant (-),
- ΔT – temperature change (°C),
- $\Delta \varepsilon$ – strain change (με).

The measurement parameters can be set in the reflectometer software during data post-processing. The measuring section length, the base of a single virtual gauge along the length and the spacing of these gauges are defined. Graphical interpretation of the parameters chosen for further analysis is shown in the Fig. 8.

For all tests and measurements described hereafter, optical backscatter reflectometer OBR4600 by Luna Innovations was applied (Fig. 9a). Selected measuring parameters important for data analysis are summarized in the Table 1. Due to the application of multiple fibre optic traces inside the composite specimens, an optical switch was used for measurements, significantly accelerating and improving the course of laboratory tests (Fig. 9b).

4. DFOS system validation on FRP laminates

4.1. Material and specimens

The rectangular composite specimens with the width of 25 mm and the thickness of 2 mm, cut from a laminate, were prepared for axial tensile tests. The composite tabs were glued to the specimens' surface to facilitate the correct anchoring in the jaws of the testing machine and to determine the measuring section between the tabs with the length of 150 mm. The most important part of the specimen was the optical fibre embedded in the centre of the cross section along the entire length of the specimen, so enabling to measure strains directly between the tabs. The optical fibres were installed on the specimens' surface in two ways: by bonding them along entire length of 100 mm by two-component epoxy glue and by spot attaching with cyano-acrylic glue in two points at a

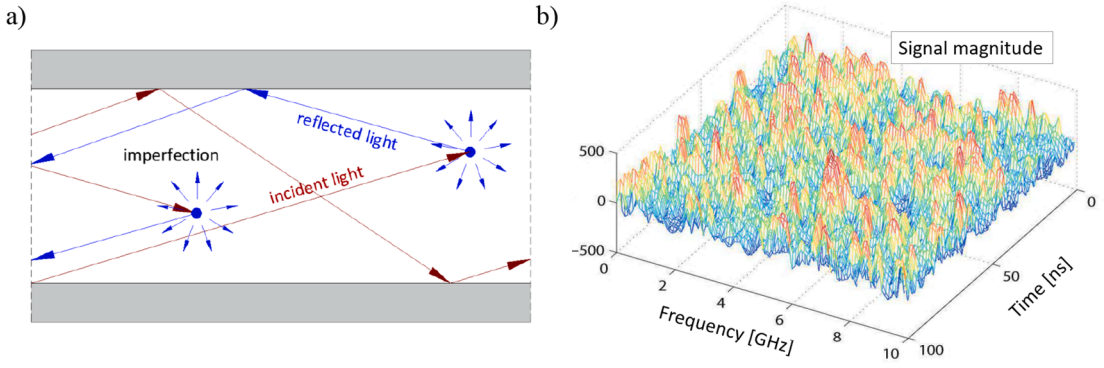

Fig. 7. a) The simplified idea of Rayleigh scattering phenomena; b) exemplary Rayleigh scattering spectrum as a random but constant fingerprint of the fibre [34].

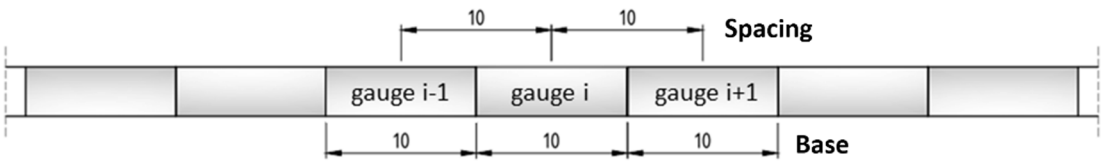

Fig. 8. Parameters of distributed fibre optic measurements (both gauge's spacing and measuring base set to 10 mm).

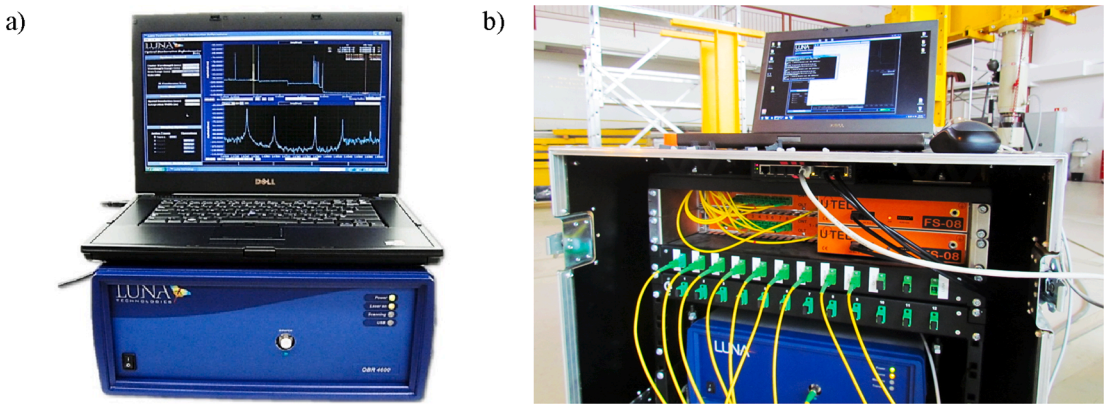

Fig. 9. a) The view of optical backscatter reflectometer OBR4600 [48]; b) the view of the reflectometer and optical switch during laboratory measurements.

Table 1
Selected parameters for static DFOS measurements.

Parameter	Value	Unit
Distance range (standard mode)	up to 70	m
Spatial resolution (gauge spacing)	10	mm
Gauge length	10	mm
Strain measurement resolution	±1,0	mm

distance of 100 mm. In this second way strains should be averaged along entire length, so their profile should be represented by a straight line. Details of the laminate specimen are presented in Fig. 10.

Depending on the specimen, optical fibres were installed on one or two surfaces of the specimen. When only one side strains were measured by DFOS, the second side was equipped with the reference foil strain gauge with 10 mm base, glued with cyano-acrylic adhesive to the surface of the specimens. Fig. 11a shows the exemplary specimens during installation of the optical fibres on their surfaces and Fig. 11b shows the close up for the glass high temperature tubes, which protect the internal fibre on the edge of the specimen.

4.2. Axial tensile tests

The axial tests were carried out in the testing machine (Instron 1200 kN - J1D). The load was applied at a speed of 10 kN/min. Due to the application of the optical reflectometer for static measurement, the loading was increased in steps of 5 kN. After reaching the respective load value, the testing machine was stopped for the DFOS measurement. The application of an optical switch (Fig. 12a) allows the measurement to be done automatically within the defined number of channels (both for the internal as well as surface fibres). The strains were recorded continuously by both methods (DFOS and foil gauges) during the test with the frequency of 10 Hz.

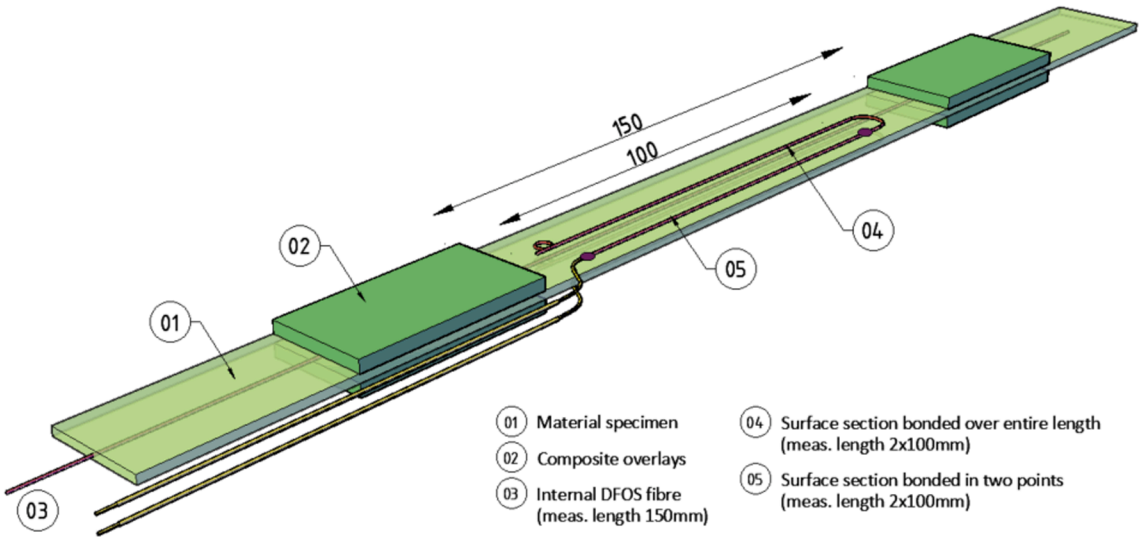

Fig. 10. The view of the composite laminate specimen for axial tensile test with optical fibres integrated inside the laminate as well as bonded on its both surfaces.

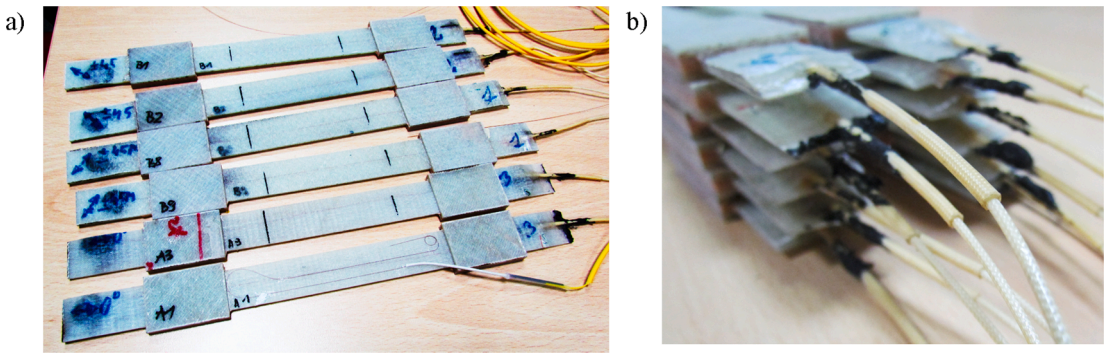

Fig. 11. a) The view of the specimens for axial tensile tests during installation of the optical fibres on surface; b) the close up to protection of internal optical fibre by high temperature tubes.

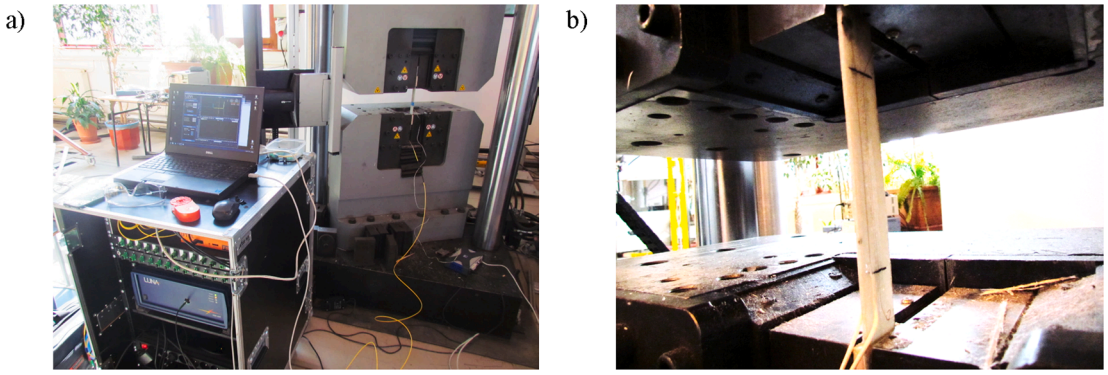

Fig. 12. a) Measurement setup with reflectometer ad optical switch during research; b) the close-up to the composite specimen during axial tensile test.

4.3. Results and discussion

In total, over a dozen laminate specimens were tested; however, only exemplary results for a representative specimen are presented and discussed hereafter. Fig. 13a shows the strain distribution measured by the internal fibre in subsequent load-steps along the entire measuring length between the tabs. Accurate strain recording was possible until the specimen failed; the maximum strain measured in the axial tensile tests was 2.8%, i.e. 28000 με. Also, the effect of the tabs crimping was observed, causing that strains are the highest in the middle of the specimen and the lowest near to the tabs. Fig. 13b shows the maximum strains measured in the mid of the specimen for a given axial load values.

Accurate measurement using surface optical fibres was possibly only in the range of strains not exceeding 1%. Similar results were obtained by both continuously-bonded as well as internal fibre (Fig. 14a) However, in the latter case the strain profile could be analysed in detail, while spot-attached fibre averaged strains along the entire measuring length. Thus, straight sections presented in Fig. 14b represent the mean strain values for the given load. The reasons why surface fibres were not able to measure strain accurately in the full range are as follows:

- breakage of the fibre's primary coating initiated by a notch at the edge of the cyano-acrylate adhesive (for spot-attached fibre);
- partial debonding of the two-component epoxy, preventing the appropriate strain transfer from the composite specimen to the measuring fibre (for continuously-bonded fibre).

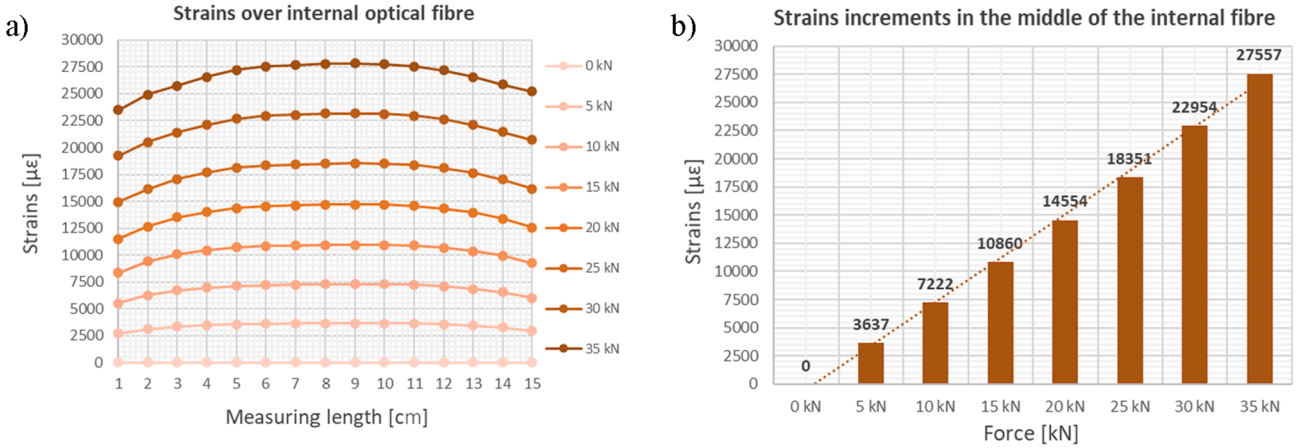

Fig. 13. Exemplary result of composite strain measurement by integrated (internal) optical fibre: a) distribution along length; b) maximum values in the middle of the specimen.

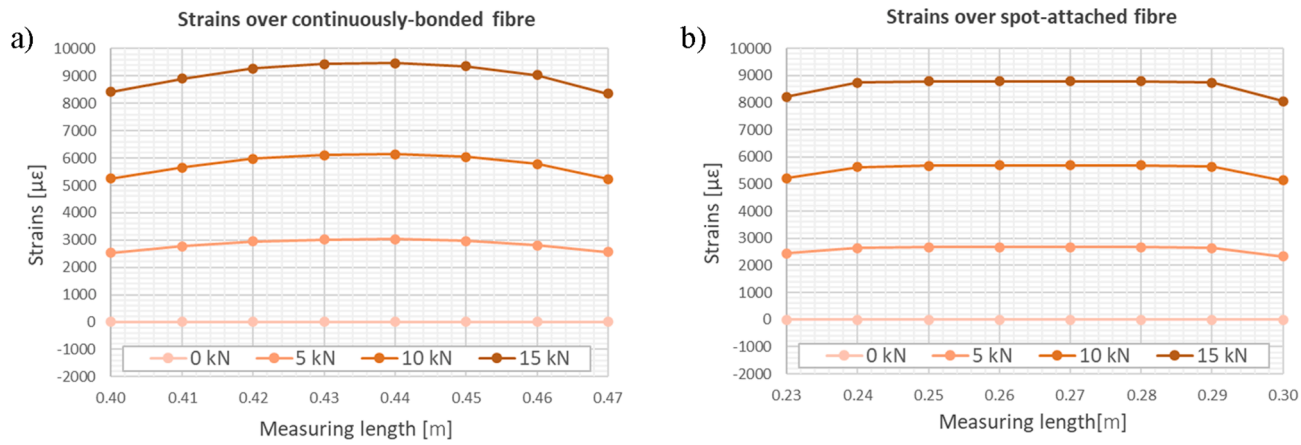

Fig. 14. Exemplary result of composite strain distributions measured by surface optical fibre: a) continuously bonded; b) spot-attached.

The last meaningful reading by surface-mounted fibres were obtained for the load of 15 kN, while internal optical fibre worked accurately up to the load of 35 kN (Fig. 15). DFOS measurement was also compared with the reference foil strain gauge readings, which withstood the load of 20 kN, corresponding to the strain of approx. 1.4%. The last meaningful measurement was obtained for the load of 25 kN (strain of 1,8%) but it was just before the gauge's failure and this record does not reflect the real behaviour of the specimen.

The laminate axial tests allowed for a preliminary assessment of the effectiveness of the proposed measuring methods by means of optical fibres integrated with the composite. This measurement method does not require surface installation (elimination of adhesive's debonding and cracking phenomena) and thus allows the strain to be measured in the full range until the specimen failure. Integration of the fibre inside the composite means that the sensor is naturally protected against mechanical damages.

5. DFOS system validation on FRP composite beam

5.1. Material and specimen

The second part of the research was the three-point bending test carried out on a beam cut from the full-scale composite panel (Fig. 16). Besides the PUR foam core, the beam contained one concrete core element, which was provided as part of a system to facilitate deck-girder connection. In this case it was decided to install optical fibres in the longitudinal direction only. The optical fibres were installed both in the lower and upper face laminates (1, 2, 3, 4) in four longitudinal sections (A, B, C, D) of the beam– see details in Fig. 16a. Longitudinal fibres were arranged with loops enabling the measurements to be done from both ends of the fibre and minimizing the risk of losing information. Embedding the fibres in the extreme positions of a given laminate (far from its neutral axis) allowed to measure not only axial strains, but also bending effects. Finally, the vertical displacements of the composite beam could be calculated in reference to zero reading – see chapter 5.5.

Additionally, one optical fibre was arranged in the six ribs of the core, localized directly under the loading. In order to protect the optical fibre on the edge between adjacent ribs, special incisions were made to allow for gentle bending of the optical fibre. The fibres left the core ribs and the beam through the layers of the upper laminate.

5.2. Three-point bending test

The composite beam was tested in three-point bending scheme in the testing machine (Instron Schenck 630 kN) The beam was supported by steel rollers at a distance of 960 mm (Fig. 16, Fig. 17a). The load was applied statically in the beam's midspan by a steel traverse of 60 mm width. The traverse was put on upper face by means of an epoxy layer, which aim was to level the upper surface enabling the load to be transferred uniformly. The load was applied at a speed of 1 mm/min.

DFOS measurements were performed step by step at the selected load levels (after stopping the testing machine). Nine measuring channels were used (eight for longitudinal section and one for the fibre installed within the core). Analogously like in the laminate tests, optical switch was applied to speed up the readings. The record taken at 250 kN was the last one made before the failure of the beam. The course of the experiment recorded by the testing machine in the form of the piston's displacements and the load values is presented in Fig. 17b.

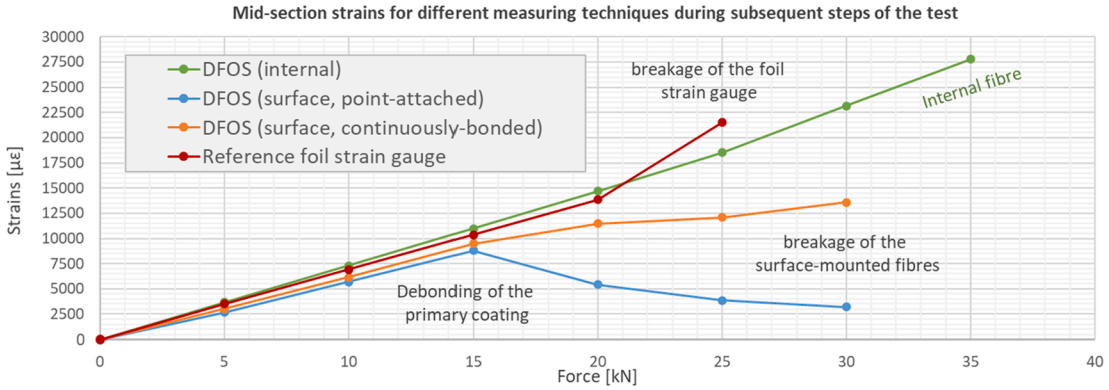

Fig. 15. Exemplary results of strains in the middle of the specimen measured by integrated (internal) optical fibre, surface-mounted fibres as well as by reference foil strain gauges.

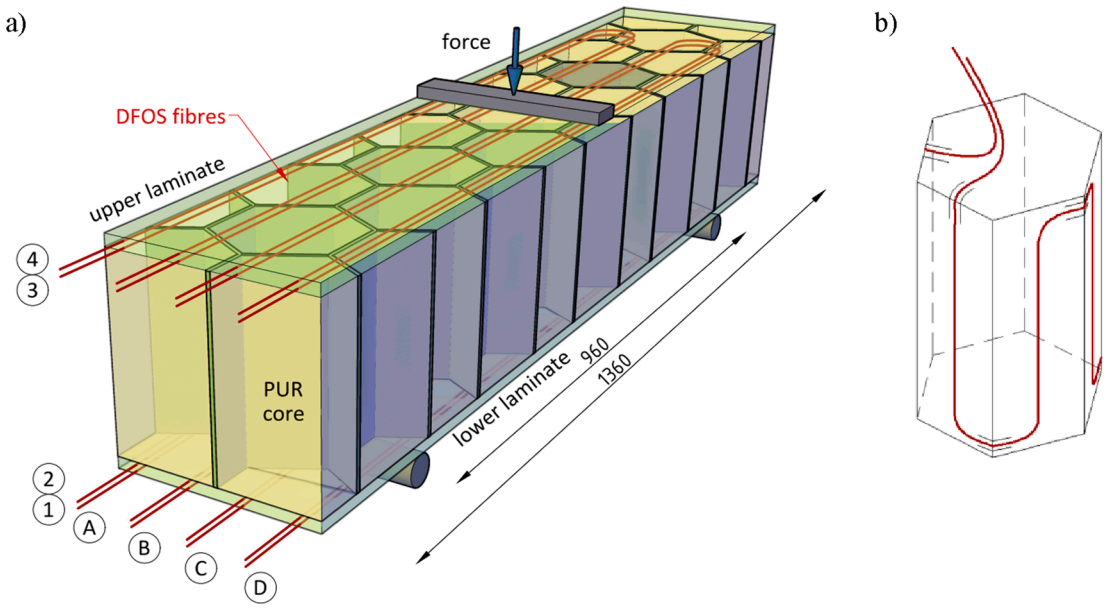

Fig. 16. Arrangement of optical fibres integrated with faces of the beam: a) inside the lower and upper laminate of the specimen; b) within the core ribs.

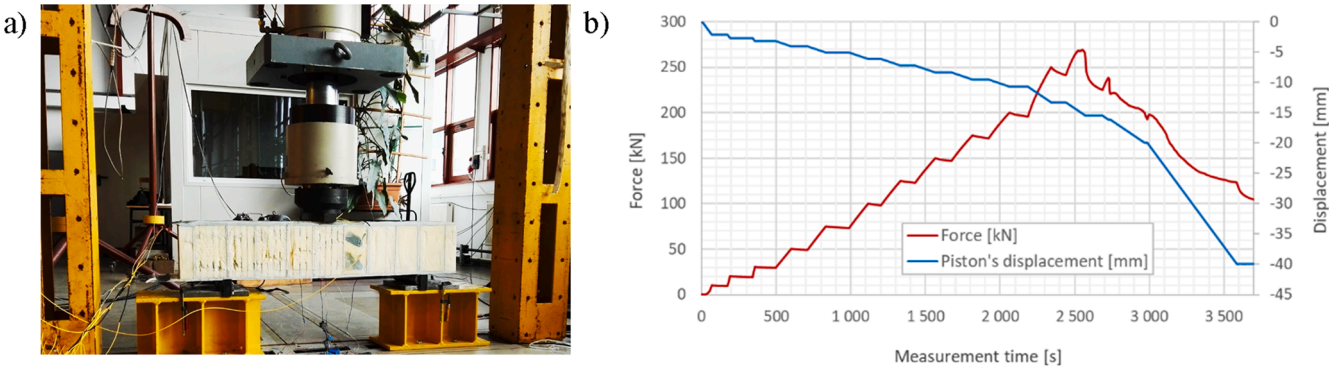

Fig. 17. a) The view of the beam during three-point bending test; b) force and displacement values recorded by the testing machine during loading.

The failure of the specimen was accompanied by cracking related to the delamination of the upper laminate. Due to high load applied directly to the upper face, local deformations of the upper laminate were clearly observed. It was the main reason of the delamination of vertical ribs, located in the immediate vicinity of the loaded area (Fig. 18a). Significant differences in the behaviour of the lower laminate were visible as compared to the upper one (Fig. 18b). The detailed analysis of these differences can be carried out based on numerical simulation and DFOS measurement.

5.3. *Numerical simulation*

The structural behaviour of the beam specimen cut from the composite panel was analysed also by numerical simulation based on the finite element method (FEM) in SOFiSTiK code. FE model of the beam was prepared using shell and brick finite elements (Fig. 19a), setting the mesh density at 0.02 m after convergence analysis. All face and rib laminates were modelled by four-node shell elements. Elements were described as multilayer material made of several, separate layers,

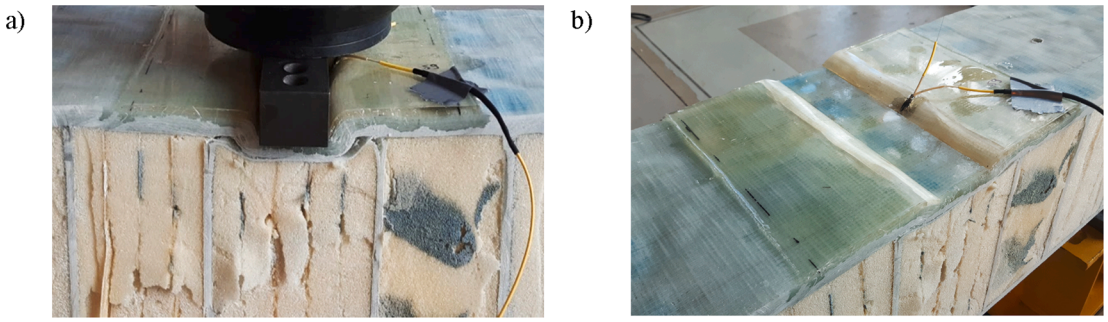

Fig. 18. The view of the beam after failure: a) delamination of the upper laminate and vertical ribs in the loading area; b) general view of the deformed upper laminate.

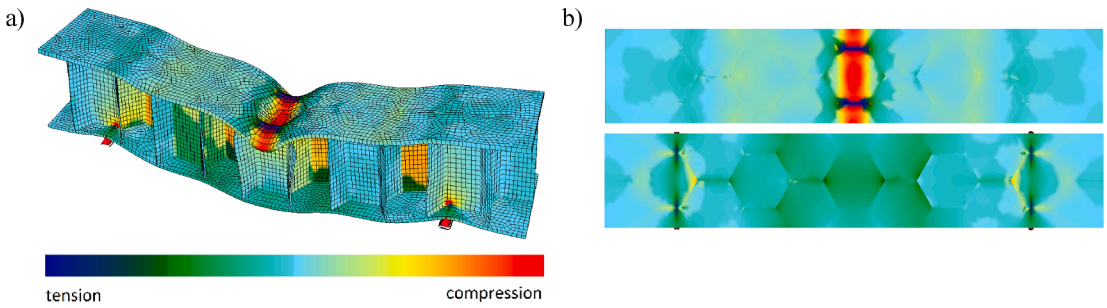

Fig. 19. Numerical simulation of the beam: a) the view of deformed model; b) strain maps of the upper and the lower face laminates.

according to stack sequence in each laminate. Parameters for each layer were determined by material testing. Laminate parameters for finite shell element were calculated based on classical laminate theory in SOFiSTiK code. Additional concrete core element was modelled by 8-node solid elements with isotropic concrete material. The final model consisted of 21 020 nodes, 12 364 shell elements and 2 528 brick elements.

Both materials: FRP and concrete were modelled as ideally elastic material with the engineering constants from material tests (Table 2). The resultant properties for the finite elements modelling multilayer laminates were the resultant of properties of individual layers, taking into account their orientation and determined according to the classical lamination theory. The load was modelled as uniform pressure applied on a contact area of 60 × 260 mm.

Fig. 19b shows strain maps obtained for the top layer of the upper laminate and the bottom layer of the lower laminate, showing the obvious differences resulting from the applied static and load scheme. Detailed data are presented in the following subsections in comparison with the DFOS results.

5.4. Results and discussion - strains

The exemplary results of DFOS measurement and FEM analysis are presented and discussed hereafter, showing the main advantages of the applied measurement method. Analysis and calculations performed for longitudinal section B are shown (Fig. 16), but the findings are also valid for all other measuring sections of the beam.

Strain distributions measured by the optical fibres embedded inside the laminates in the subsequent load steps are presented in Fig. 20. The values measured at load of 250 kN just before failure of the specimen are highlighted in red. Fig. 20a shows strains for the bottom layer of the lower laminate, while Fig. 20b for the top layer of the upper laminate. Shapes of strain profiles were also compared with the results of numerical simulations. The comparison showed that the measurements made along the entire length of the tested element are highly consistent with the results obtained from the numerical model. Not only the global response, but also local effects were observed, what is impossible to capture when using spot strain measurement.

Distributed strain measurement can change the conventional way of analysing structural members, extending the analysis from one domain (time) to two domains (both time and length). Thus, the results can be presented on spatial visualizations (Fig. 21a and b).

The strain profiles for the composite beams are characterized by a great variety and large gradients along even small length (Fig. 21). This is a perfect example of the limitations of conventional spot strain gauges, which average strains along the base in one point of the element or structure. Even the small change in the spot gauge location will cause the significant change in the measured values and thus the results interpretation. That is why it should be performed with the special caution and precision. Distributed strain sensing completely eliminates this problem, showing the full and comprehensive picture of the structural behaviour not only on the surface, but also inside the laminate. Because of the negligible costs of the optical fibres there is no need to limit the number of measuring sections within the composite laminates.

Table 2
Engineering constants of materials adopted in the simulation.

Material	Longitudinal modulus of elasticity [GPa] E_1	Transverse modulus of elasticity [GPa] E_2	In-plane shear modulus [GPa] G_{12}	Longitudinal Poisson's Ratio [–] ν_{12}
U-E	35,48	10,46	3,14	0,24
B-E	24,65	21,44	2,83	0,15
X-E	24,25	24,25	2,75	0,25
Concrete	28,85	28,85	12,02	0,20

5.5. Results and discussion - displacement

The measured strain distributions in the subsequent load stages can be used for the assessment of displacements, treated as changes in the laminates' shape relatively to the original shape before loading. One of the methods can be the calibration of numerical model by comparing DFOS strain results with FEM simulation and then adjusting the FE model parameters (e.g. stiffens, thicknesses, boundary conditions) to obtain better compliance. Such validated FE model, with increased reliability, can be further used to estimate various parameters of the beam, e.g. displacements, with better accuracy than before calibration.

However, this is very simplified approach. Much better and accurate solution is based on direct calculation of the displacements. It is possible knowing strain profiles along entire measuring length, the location of optical fibres relative to the neutral axis of the respective laminate (in this case bottom and top layers of the laminate), DFOS spatial resolution (10 mm) and boundary conditions – see Eq. (2):

$$u_v = f(\varepsilon_B, \varepsilon_T, H, b, bc) \tag{2}$$

where

- u_v – vertical displacement profile over length (mm);
- ε_B – strain profile along the bottom layer of the laminate (με);
- ε_T – strain profile along the top layer of the laminate (με);
- H – distance between the bottom and top optical fibre, which is assumed to be constant during the specimen deformation (mm);
- b – spatial resolution (mm) (base length of individual gauges along length);
- bc – boundary conditions (e.g. for simply-supported beam displacements at the supports equal zero).

What is very important, this algorithm, unlike the deflection equation, doesn't require the knowledge about material properties (e.g. elasticity modulus) and can be apply also in the range of large displacements. It is based only on geometrical analysis of the chain of virtual gauges with the base equal to the defined spatial resolution and the height equal to the spacing of the optical fibres (lower and upper). In

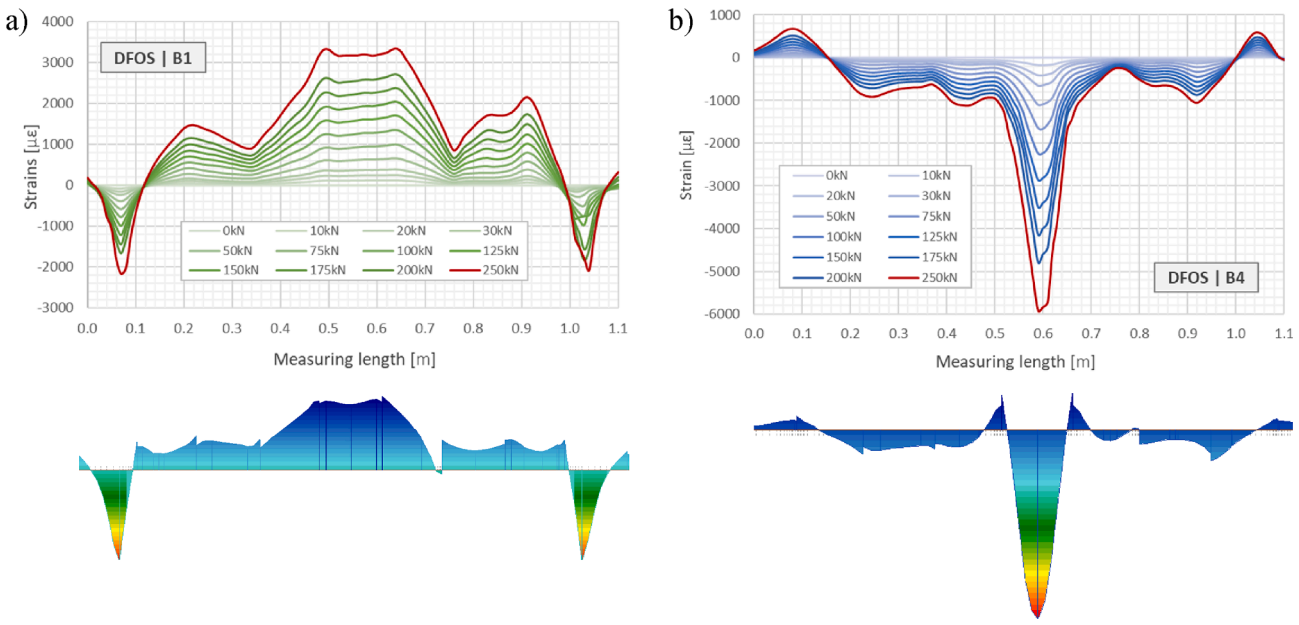

Fig. 20. Strain distributions along measuring length in the subsequent load steps qualitatively compared to the results of numerical simulation for: a) bottom layer of the lower laminate; b) top layer of the upper laminate.

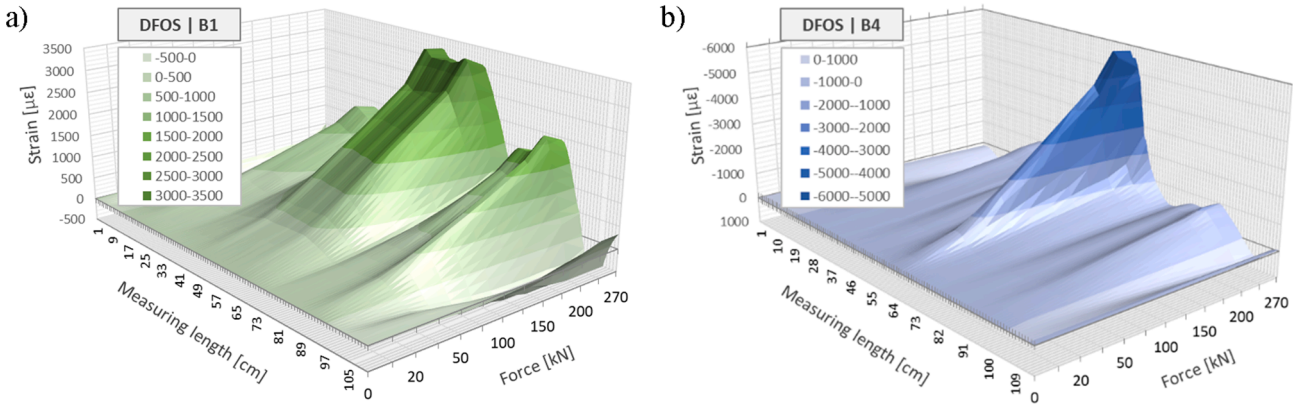

Fig. 21. Spatial visualization of strain distributions in the measuring length and load domain for: a) bottom surface of the lower laminate; b) top surface of the upper laminate.

the initial configuration (zero state) such a gauge is represented by a rectangle, but after deformation it takes the form of the trapeze (Fig. 22). Displacements are calculated for individual gauges and then summed up to produce the displacement profile along entire measuring length.

Displacements calculated for both the lower and upper composite laminates of the beam loaded in three-point bending test are presented in Fig. 23a and 23b, respectively. Because of the local pressure caused by the load applied to the upper laminate, its displacements are of the greater values and gradients, especially in the mid-section. Very good qualitative agreement was obtained with numerical simulations.

Quantitative comparison between the DFOS data, both the strain and displacements, with finite element model shows that the FE model overestimates the results. It is caused mainly due to the fact, that in the FE model the designed (assumed) geometrical (e.g. thickness) and physical (e.g. elasticity modulus) parameters were used. They should be replaced by the data from material testing and beam's as-built inventory as well as calibration based on the measurements [49].

6. Conclusions

The paper describes the concept of the smart FRP composite bridge panel with integrated distributed fibre optic sensors (DFOS), embedded in its structure to monitor the panel's behaviour under loading, particularly to measure strains and displacements of in the innovative, continuous manner. Exemplary data of DFOS efficiency were presented, obtained from testing of the DFOS equipped specimens: the multi-layered laminates in the axial tensile tests as well as the beam cut from the panel in three-point bending test. The technical aspects of this relatively new measurement technique such as installation of the optical fibres inside the laminates, protection within the sensitive areas, termination, splicing and calibration of the applied optical fibres were also discussed. Finally, the overall accuracy and reliability of the DFOS measurement system were revealed.

It should be emphasized that the presented study was only preliminary one, preparing for further works including the analysis of full-scale bridge panels. The initial works on the smart composite deck panels discussed in this paper allowed for verification of the effectiveness of the proposed measurement method. The DFOS measurements and accompanying analyses led the authors to the following conclusions:

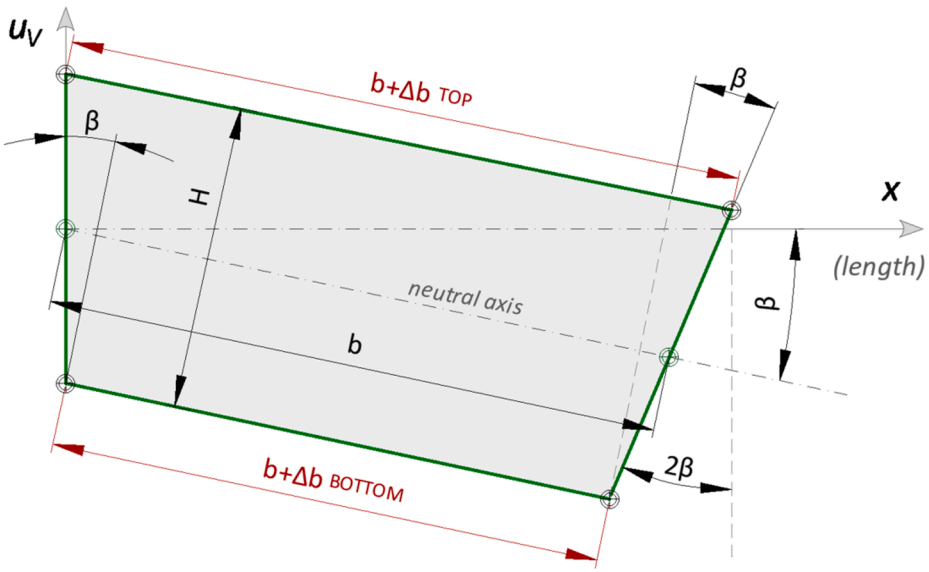

Fig. 22. Geometry of the deformed individual virtual gauge with the initial base *b*, created from two optical fibres with a spacing of *H*.

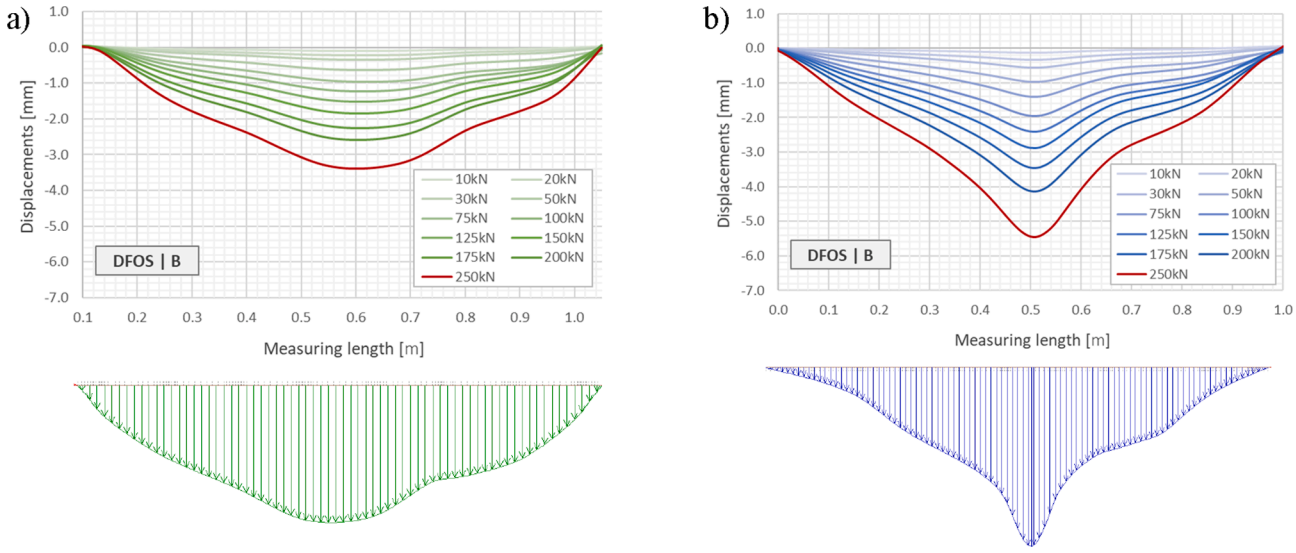

Fig. 23. Displacement profiles along measuring length of the beam in the subsequent load steps qualitatively compared to the results of numerical analysis for: a) the lower laminate; b) the upper laminate.

- the technical feasibility of strain and displacement measurements with DFOS monitoring system dedicated to the smart composite deck panel was confirmed;
- all optical fibres did not brake under load and production process (VARTM infusion) did not cause any local imperfections, that could hinder or prevent accurate measurement;
- the application of the common telecommunication optical fibres in their primary acrylic coating integrated inside the composite laminates was effective for DFOS measurement, even in the case of extremely large strains (2.8%); owing to the full integration of the fibre with the laminates, strains were measured very accurately;
- installation of the DFOS measuring system before the infusion allowed for the measurement to be made from a really zero state: taking into account strains induced during production, transportation, construction and exploitation; such comprehensive information is not available for conventional measurement approach, were sensors are usually surface-mounted on the ready structures;
- it is advantageous, reasonable and feasible to install the optical fibres within at least two layers of the laminate, at known spacing; it allows for analysing not only strains but also for calculation of displacements (shapes) of the structural element based only on geometrical relations; initial test provided within this research allowed for positive verification of the proposed approach;
- DFOS measurements shown good compliance with reference measurement results, both for strains and displacements;
- numerical simulations based on FE model with nominal geometrical and physical parameters overestimated the DFOS results on average by 20%; the obtained DFOS measurements can be used for FE model calibration and thus to optimize both designing and construction process.

The concept of the precast, smart composite deck panels dedicated for bridge engineering, integrated with advanced distributed fibre optic system for strain and displacements measurements and monitoring is very promising in the context of the performance, reliability,

maintenance and durability of bridges. Works, measurements and analysis described in this paper will contribute to the development of smart composite structures, solving some technological, production, measurement and calculation problems related to integration of optical fibres inside the composite material.

CRediT authorship contribution statement

Maciej Kulpa: Conceptualization, Methodology, Formal analysis, Investigation, Project administration, Writing - review & editing, Funding acquisition. **Tomasz Howiacki:** Software, Validation, Formal analysis, Investigation, Visualization, Writing - original draft. **Agnieszka Wiater:** Investigation, Formal analysis, Resources, Writing - original draft. **Tomasz Siwowski:** Conceptualization, Methodology, Resources, Supervision. **Rafał Sieńko:** Conceptualization, Methodology, Resources, Supervision.

Declaration of Competing Interest

The authors declare that they have no known competing financial interests or personal relationships that could have appeared to influence the work reported in this paper.

Acknowledgements

The research described within this paper was performed within the R&D project: "*OptiDeck - Intelligent FRP deck system for construction and rehabilitation of road bridge structures, equipped with fibre optic sensors for structural health monitoring and bridge load controlling*" carried out by Rzeszow University of Technology, Poland. This project was funded by the grant of the National Centre for Research and Development (Poland) within the framework of the LIDER Program.

References

[1] L.C. Holloway, P.R. Head, Advanced Polymer Composites and Polymers in the Civil Infrastructure, Elsevier Science Ltd, London, 2001.
[2] T. Keller, Use of fibre reinforced polymers in bridge construction, Structural Engineering Documents SED 7, International Association for Bridge and Structural Engineering (IABSE), Zurich, 2003.
[3] M. Zoghi (Ed.), The International Handbook of FRP Composites in Civil Engineering, CRC Press, Taylor & Francis Group LLC, Boca Raton, 2014.
[4] T. Siwowski, FRP composite bridges: Structural shaping, design, testing, Publisher: Wydawnictwo Naukowe PWN, Warszawa, ISBN: 978-83-01-19921-0.
[5] T. Siwowski, M. Kulpa, M. Rajchel, P. Poneta, Design, manufacturing and structural testing of an all-composite FRP bridge girder, Compos. Struct. 206 (15) (December 2018) 814–827.
[6] M. Kulpa, T. Siwowski, Stiffness and strength evaluation of a novel FRP sandwich panel for bridge redecking, Compos. B Eng. 167 (15) (June 2019) 207–220.
[7] T. Siwowski, M. Rajchel, Structural performance of a hybrid FRP composite – lightweight concrete bridge girder, Compos. B 174 (2019), 107055.
[8] J. Chróścielewski, M. Miśkiewicz, Ł. Pyrzowski, B. Sobczyk, K. Wilde, A novel sandwich footbridge - practical application of laminated composites in bridge design and in situ measurements of static response, Compos B Eng 126 (2017) 153–161.
[9] W. Lestari, P. Qiao, Damage detection of fiber-reinforced polymer honeycomb sandwich beams, Compos. Struct. 67 (2005) 365–373.
[10] Udaya B. Halabe, Archana Vasudevan, Powsiri Klinkhachorn, Hota V.S. GangaRao, Detection of subsurface defects in fiber reinforced polymer composite bridge decks using digital infrared thermography, Nondestructive Testing And Evaluation 22 (2-3) (2007) 155–175.
[11] S. Gholizadeh, A review of non-destructive testing methods of composite materials, Procedia Struct. Integrity 1 (2016) 050–057.
[12] D.N. Farhey, Instrumentation system performance for long-term bridge health monitoring, Struct. Health Monit. 5 (2) (2006) 143–153, https://doi.org/10.1177/1475921706057986.
[13] Hong Guan, Vistasp M. Karbhari, Charles S. Sikorsky. Long-term structural health monitoring system for a FRP composite highway bridge structure, J. Intell. Mater. Syst. Struct., 18(8), 2007.
[14] Bryan R. Loyola, Valeria La Saponara, Kenneth J. Loh, In situ strain monitoring of fiber-reinforced polymers using embedded piezoresistive nanocomposites, J. Mater. Sci. 45 (2010) 6786–6798.
[15] W.M. Sebastian, M. Johnson, Interpretation of sensor data from in situ tests on a transversely bonded fibre-reinforced polymer road bridge, Struct. Health Monit. (2018), https://doi.org/10.1177/1475921718779403.
[16] E.A. Dibiago, Case study of Vibrating-Wire Sensors That Have Vibrated Continuously For 27 Years, Field Measurements in Geomechanics, September 15-18, 2003.
[17] M. Guerrieri, G. Parla, C. Celauro, Digital image analysis technique for measuring railway track defects and ballast gradation, Measurement 113 (January 2018) 137–147.
[18] C.Z. Dong, X.W. Ye, T. Jin, Identification of structural dynamic characteristics based on machine vision technology, Measurement 126 (2018) 405–416.
[19] G. Li, Q. Tan, Q. Sun, Y. Hou, Normal strain measurement by machine vision, Measurement 50 (2014) 106–114.
[20] R. Bogue, Recent developments in MEMS sensors: A review of applications, markets and technologies, Sens. Rev. 33 (4) (September 2013), https://doi.org/10.1108/SR-05-2013-678.
[21] J. Zhu, X. Liu, Q. Shi, et al., Development trends and perspectives of future sensors and MEMS/NEMS, Micromachines (Basel). 11 (1) (2020 Jan) 7, https://doi.org/10.3390/mi11010007.
[22] A.M. Abazari, S.M. Safavi, G. Zezazadeh, M. Fathalilou, Couple stress effect on micro/nanocantilever-based capacitive gas sensor, Int. J. Eng. 29 (6) (2016) 852–861.
[23] N. Aisah, L. Aprilia, R. Nuryadi, Piezoresistive microcantilever-based gas sensor using dynamic mode measurement, in: 2013 International Conference on QiR, Yogyakarta, 2013, pp. 5-8, doi: 10.1109/QiR.2013.6632525.
[24] Y.L. Xu, Y. Xia, Structural Health Monitoring of Long-Span Suspension Bridges, Spon Press, London and New York, 2012.
[25] B. Glišić, D. Inaudi, Fibre Optic Methods for Structural Health Monitoring, Wiley, 2007.
[26] R. Measures, Structural Monitoring with Fiber Optic Technology, Academic Press, 2001.
[27] C. Gheorghiu, P. Labossiere, J. Proulx, Fiber optic sensors for strain measurement of CFRP-strengthened RC Beams, Struct. Health Monit. 4 (2005) 67, https://doi.org/10.1177/1475921705049754.
[28] M. Amanzadeh, S.M. Aminossadati, M.S. Kizil, A.D. Rakić, Recent developments in fibre optic shape sensing, Measurement 128 (2018) 119–137.
[29] A. Piccolo, S. Delepine-Lesoille, F. Bumbieler, J. Zghondi, Y. Lecieux, D. Leduc, P. Teixeira, O. Gay, Tunnel monitoring: Performances of several innovative shape sensing systems, Technological Innovations in Nuclear Civil Engineering, France, Paris-Saclay – 2018, August 29.
[30] D.-P. Zhou, W. Li, L. Chen, X. Bao, Distributed temperature and strain discrimination with stimulated Brillouin scattering and Rayleigh backscatter in an optical fiber, Sensors 13 (2013) 1836–1845, https://doi.org/10.3390/s130201836.
[31] J.M. López –Higuera, L. Rodriguez, A. Quintela, et al. Fiber optic sensors in structural health monitoring, J. Lightwave Technol. 2011, 29(4): 587–608.
[32] D. Samiec, Distributed fibre-optic temperature and strain measurement with extremely high spatial resolution, Photonic International, 2012.
[33] M. Weisbrich, K. Holschemacher, Comparison between different fiber caotings and adhesives on steel surfaces for distributed optical strain measurements based on Rayleigh backscattering, J. Sens. Sens. Syst. 7 (2018) 601–608.
[34] R. Sieńko, Ł. Bednarski, T. Howiacki, About distributed internal and surface strain measurements within prestressed concrete truck scale platforms, in: 3rd World Multidisciplinary Civil Engineering - Architecture - Urban Planning Symposium WMCAUS, Prague, Czech Republic, 18-22 June 2018.
[35] M. Ramakrishnan, G. Rajan, Y. Semenova, G. Farrell, Overview of fiber optic sensor technologies for strain/temperature sensing applications in composite materials, Sensors 16 (2016) 99, https://doi.org/10.3390/s16010099.
[36] T. Siwowski, D. Kaleta, M. Rajchel, Structural behaviour of an all-composite road bridge, Compos. Struct. 192 (2018) 555–567.
[37] C. Schilder, M. Schukar, M. Steffen, K. Krebber, Structural health monitoring of composite structures by distributed fibre optic sensors, in: 5th International Symposium on NDT in Aerospace, 13-15th November 2013, Singapore.
[38] T. Siwowski, M. Rajchel, R. Sieńko, Ł. Bednarski, Smart monitoring of the FRP composite bridge with distributed fibre optic sensors, in: 9th International Conference on Fibre-Reinforced Polymer (FRP) Composites in Civil Engineering (CICE 2018), Paris, 2018.
[39] M.R. Gurvich, M. Urban, N. Bordick, Experimental investigations in embedded sensing for structural health monitoring of composite components in aerospace vehicles, Compos. B Eng. 71 (March 2015) 15.
[40] Y.W.S. Chan, Z. Zhou, Advances of FRP-based smart components and structures, Pacific Science Review 16, 2014.
[41] G. Zhou, L. Sim, Damage detection and assessment in fibre-reinforced composite structures with embedded fibre optic sensors-review, Smart Mater. Struct. 11(6), 2002.
[42] K. Lau, L. Yuan, L. Zhou, J. Wu, Ch. Woo, Strain monitoring in FRP laminates and concrete beams using FBG sensors, Compos. Struct. (2001).
[43] L. Meng, L. Wang, Y. Hou, G. Yan, A research on low modulus distributed fiber optical sensor for pavement material strain monitoring, Sensors 17 (2017) 2386.
[44] D.S. Raffaella, Fibre optic sensors for structural health monitoring of aircraft composite structures, Recent Adv. Appl., Sens. 15 (2015).
[45] A. Güemes, A. Fernández-López, B. Soller, Optical fiber distributed sensing – physical principles and applications, Struct. Health Monit. Int. J. 9 (3) (2010) 233–245.
[46] D. Gifford, B. Soller, M. Wolfe, et al. Distributed fiber-optic sensing using Rayleigh backscatter, in: European Conference on Optical Communications (ECOC) Technical Digest, Glasgow, Scotland, 2005.

[47] K. Kishida, A. Guzik, Study of optical fibers strain-temperature sensitivities using hybrid Brillouin-Rayleigh system, Photon. Sens. (2014), https://doi.org/10.1007/s13320-013-0136-1.
[48] Luna Technologies, Optical Backscatter Reflectometer Model 4600, User Guide 6, OBR 4600 Software 3.10.1, 2013.
[49] T. Howiacki, R. Sieńko, M. Sýkora, Reliability analysis of serviceability of long span roof using measurements and FEM model, AIP Conference Proceedings 2116, 450078 (2019), 24 July 2019, https://doi.org/10.1063/1.5114545.